A method for measuring magnetic fields in sunspots using Zeeman-broadened absorption lines

Benjamin Oostra

Citation: American Journal of Physics **85**, 295 (2017); doi: 10.1119/1.4975109
View online: http://dx.doi.org/10.1119/1.4975109
View Table of Contents: http://aapt.scitation.org/toc/ajp/85/4
Published by the American Association of Physics Teachers

A method for measuring magnetic fields in sunspots using Zeeman-broadened absorption lines

Benjamin Oostra
Departamento de Física, Universidad de los Andes, Bogotá, Colombia

(Received 11 November 2015; accepted 16 January 2017)

We present measurements of magnetic fields in several sunspots using high-resolution spectra obtained with the ESPARTACO spectrograph at the Universidad de los Andes, with the aim to explore experimental possibilities for students. Because the Zeeman line splitting is smaller than the line width, our work only observes broadened absorption lines. This broadening, however, can be measured and suitably modeled, giving realistic quantitative results.
[http://dx.doi.org/10.1119/1.4975109]

I. INTRODUCTION

The Zeeman effect is commonly used for astronomical measurements of magnetic fields. One method is to resolve split spectral lines,[1] while another technique involves measurements of the polarization of the light.[2] Insofar as magnetic fields go, *strong* magnetic fields are normally found in sunspots. The solar magnetic field is usually below the Sun's surface (photosphere), but during epochs of increased solar activity it is common for magnetic field lines to be expelled outward into the solar corona forming spectacular loops. At the points where the field lines cross the photosphere, the convection process, which transfers heat from the solar interior to the surface, is inhibited. This causes patches of the photosphere to be cooler than the rest of the Sun's surface, producing sunspots. The gas just above a sunspot is thus embedded in a magnetic field, causing the absorption spectrum to exhibit the Zeeman Effect, which can be used to measure the field strength. Such measurements provide information on the magnetic field in the solar interior. Currently, the Sun is continually monitored by dedicated instruments like the Helioseismic and Magnetic Imager (HMI)[3] on the orbiting Solar Dynamics Observatory (SDO),[4] which, among other properties, measure magnetic fields.

When spectral lines are noticeably split by the Zeeman effect, the separation between the components may be measured directly and the field strength follows. But when the spectral resolution is just sufficient to observe a measurable line broadening (and not enough to resolve the line splitting), the process is less straightforward.

This is the case for sunspot spectra taken with the ESPARTACO spectrograph ("Espectrógrafo de Alta Resolución para Trabajos Astronómicos en Colombia") at the Astronomical Observatory of the Universidad de los Andes. This instrument,[5,6] built for student use, offers resolutions up to $\lambda/\Delta\lambda \approx 90,000$ (here, $\Delta\lambda$ is the observed width of a perfectly monochromatic spectral line); this resolution is sufficient to notice the broadening of absorption lines in sunspots, but not enough to see them split. The broadening can be measured, but this value is not equal to the Zeeman splitting value. Here, we describe a method to obtain the magnetic field strength from the broadened lines. We note that a different approach to tackle this problem, involving autocorrelation of spectra, has been recently published by Borra and Deschatelets.[7]

II. THE ZEEMAN EFFECT

In a magnetic field, an atom has a potential energy U associated with the orientation of its magnetic moment with respect to an external magnetic field B. This energy can be written as

$$U = g\, m_J \left(\frac{e\hbar}{2m}\right) B, \tag{1}$$

where e and m are the electron's charge and mass, $\hbar$ is Planck's constant, m_J is the magnetic quantum number associated with the total angular momentum (the corresponding quantum operators are J and J_z), and g is the Landé factor of that particular energy level, given by

$$g = 1 + \frac{J(J+1) + S(S+1) - L(L+1)}{2J(J+1)}. \tag{2}$$

This formula for g, where L represents the total orbital angular momentum (of the several electrons) and S the total spin, is valid only if $J \neq 0$ (and only for atoms adhering to the LS-coupling scheme). If $J = 0$ there is no energy splitting (although the magnetic moment may be non-zero) because $m_J = 0$ (recall that $m_J = J, J-1, \ldots, -J$).

When a photon is absorbed, the atom undergoes a transition between two energy levels, each of which may be split into several components by the magnetic field. In this way, several similar but distinct frequencies may be absorbed, and the absorption lines are multiples. However, transitions are not possible between any pair of sub-levels because they are subject to the selection rule

$$\Delta m_J = 0, \pm 1. \tag{3}$$

Spectral lines due to transitions with $\Delta m_J = 0$ are called π components, while lines produced when $\Delta m_J = \pm 1$ are referred to as σ components. These designations are based on the polarization.

If one of the two levels has $J = 0$, or if both levels have the same g, the selection rule implies that only three components will appear with equal separations. These are the Zeeman triplets. A particular example of this condition is called the "Normal Zeeman Effect" which occurs when both levels have $S = 0$, making $J = L$ and $g = 1$, or if one level has $J = 0$ and the other has $g = 1$.

In the general triplet case, the wavelength separation between the central π line and any of the two σ lines may be

computed using $m_J = 1$ in Eq. (1), and recalling the relation between the photon's energy E and the emitted wavelength,

$$E = \hbar\omega = \frac{2\pi\hbar c}{\lambda}. \tag{4}$$

Differentiating gives

$$\Delta E = \frac{2\pi\hbar c}{\lambda^2}\Delta\lambda, \tag{5}$$

and combining this result with Eq. (1), while taking $\Delta E = U$, we get

$$\Delta\lambda = \left(\frac{e}{4\pi m c}\right) g\,\lambda^2 B. \tag{6}$$

Most transitions, however, are not triplets and instead involve pairs of energy levels having both $J \neq 0$ and different Landé factors. These transitions exhibit more complicated splitting patterns with multiple values of $\Delta\lambda$. But all the same, if the g factors are known and the spectral lines are experimentally resolved, the several $\Delta\lambda$ may be measured and the field may be directly computed.

However, if the Zeeman splitting is smaller than the line width, the components are not resolved, and their positions cannot be accurately measured. This occurs in the case of weak magnetic fields, low-sensitivity transitions, and/or insufficient instrumental resolution. In this case, the absorption line may be broadened. Figure 1 shows this effect in two solar absorption lines, observed within and outside a sunspot. ESPARTACO can resolve line splitting in a laboratory field of 10,000 G, but not in sunspots where field strengths rarely exceed 3000 G. However, the broadening can be measured in a considerable number of lines.

The broadening is related to the average displacement of the σ components, which may be expressed in a form similar to Eq. (6) as

$$\Delta\lambda = \left(\frac{e}{4\pi m c}\right) G\,\lambda^2 B, \tag{7}$$

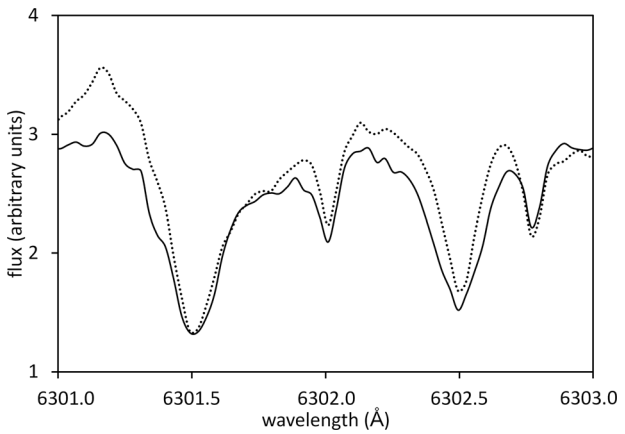

Fig. 1. A small portion of the solar spectrum obtained with ESPARTACO, showing a pair of iron absorption lines with high G values. The solid curve represents the sunspot spectrum; the dotted curve is a reference spectrum from outside the sunspot. The two smaller absorption lines (at 6302 Å and 6302.8 Å) are produced by atmospheric oxygen and are not broadened. The triplet structure of the line at 6302.5 Å is vaguely visible but not resolved. The line at 6301.5 Å splits into more than three components.

where G is known as the Landé factor for the transition, and depends on the quantum numbers of both levels. A first approximation to G is given by[8]

$$G = \left(\frac{g_1 + g_2}{2}\right) + \left(\frac{g_1 - g_2}{4}\right)[J_1(J_1+1) - J_2(J_2+1)]. \tag{8}$$

More exact values for G can be found for many spectral lines in databases like VALD[9] or Spectroweb.[10] In Zeeman triplets, this transition G factor is equal to the g factor that characterizes one or both energy levels. If G is known for a given transition and $\Delta\lambda$ is obtained from measurements, Eq. (7) can be used to obtain the magnetic field.

III. MEASUREMENT OF THE LINE BROADENING

After obtaining the spectra, the first issue is how to measure the line broadening. A first idea would be to measure the FWHM (full width at half maximum) of a certain absorption line in a sunspot spectrum, then measure the FWHM of the same line in a reference spectrum taken outside the sunspot, and finally take the difference. The difficulty of this approach is that ESPARTACO solar spectra suffer from severe modulation of the continuum (Fig. 2). This modulation is caused by intermodal interference within the optical fiber between the telescope and the spectrograph. Often the continuum does not have the same level at both sides of an absorption line (Fig. 3), so it is not clear where the "half maximum" level should be chosen.

For the process of measuring the line broadening, the following method was used. First, superpose the two spectra on a single plot, including vertical grid lines (with a spacing of about 0.01 Å) and some horizontal lines, to aid the measuring process. Second, inflate the amplitude of the sunspot spectrum until the sides of the selected spectral line become parallel. In other words, the left side of the line in the sunspot spectrum must be parallel to the left side of the same line in the reference spectrum, and the same for the right sides (see Figs. 4 and 5). This can be achieved by visual inspection, but it may be helpful to measure the broadening at several heights and assess whether or not the values show a trend.

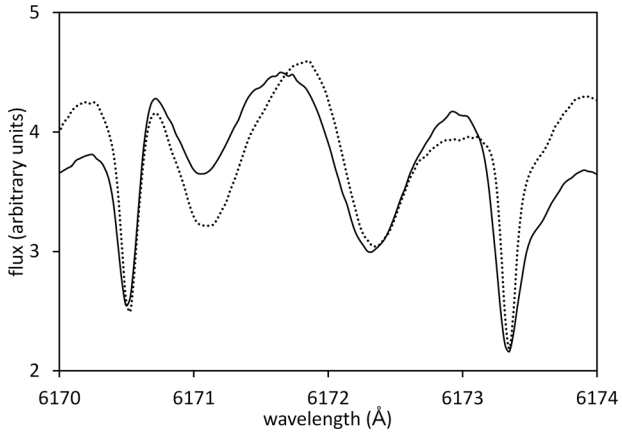

Fig. 2. Modulation of the continuum. The two sharp minima are true absorption lines, but the two waves between them are artifacts from the instrument. The solid curve represents the sunspot spectrum; the dotted curve is a reference spectrum from outside the sunspot. Notice that the line at 6173.3 Å is clearly broadened; the line at 6170.5 Å much less so.

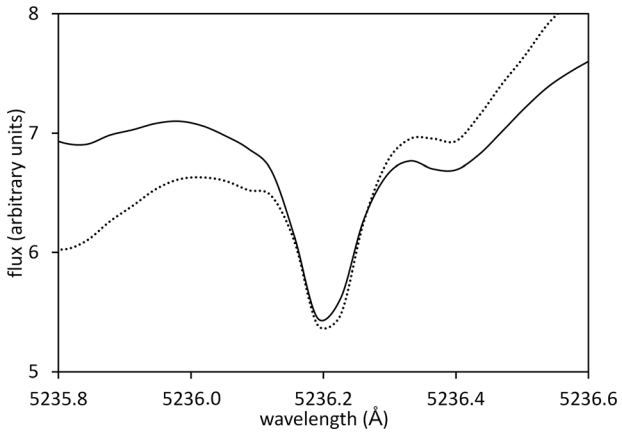

Fig. 3. Discontinuity of the continuum. The continuum spectrum does not have the same level on both sides of the absorption line. This particular line is a low-sensitivity iron absorption line. The solid curve represents the sunspot spectrum; the dotted curve is a reference spectrum from outside the sunspot.

Third, add a constant to the sunspot spectrum in order to match (as much as possible) the continuum-levels of the two spectra. When this is accomplished, the broadening can be measured without ambiguity because it is independent of the height at which it is measured. In fact, it can be measured at several levels and averaged.

The line broadening δ measured in this way is not equal to the Zeeman splitting $\Delta\lambda$ from which the magnetic field must be computed. The observed broadening may be much smaller than the theoretical splitting, depending on the width W of the absorption line. Section IV develops a relation between these three quantities for the particular case of Zeeman triplets.

IV. ZEEMAN SPLITTING FROM LINE BROADENING

We now proceed to find the relation between the measured broadening δ and the Zeeman splitting $\Delta\lambda$ for triplets. For this purpose, we construct an analytical model.

We assume spectral lines to be Gaussian-shaped, and study the superposition of three Gaussian profiles, one (the π component) remaining at the center and the other two (the σ components) shifted an amount Δ towards either side. This Δ

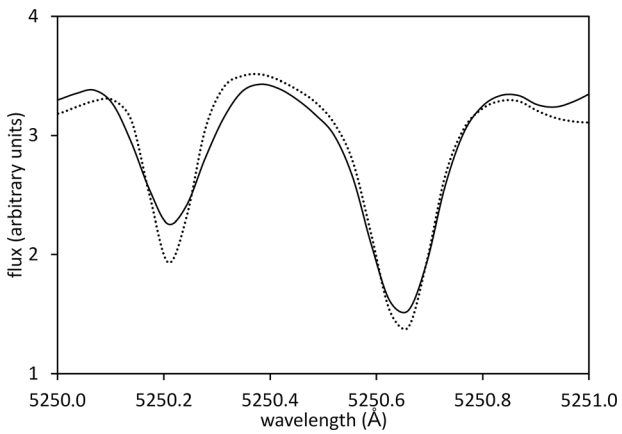

Fig. 4. The Fe I line at 5250.2 Å is very sensitive to magnetic fields. In the sunspot spectrum (solid curve), it is strongly broadened and the depth is correspondingly reduced. The dotted curve is the reference spectrum from outside the sunspot.

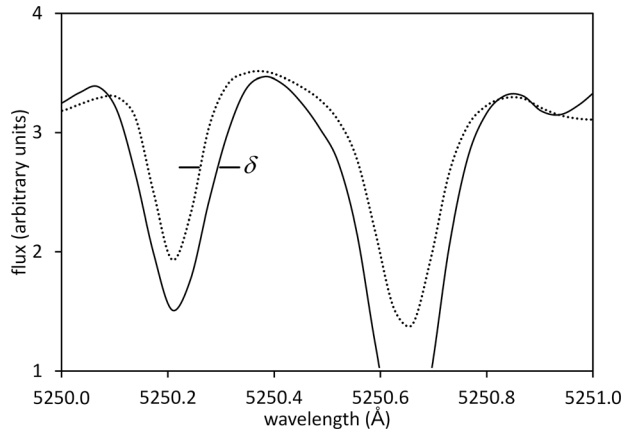

Fig. 5. The vertical scale of the sunspot spectrum has been inflated by a factor of 5/3, making the sides parallel. The broadening δ can now be measured.

represents the $\Delta\lambda$ wavelength shift. In absence of any magnetic field, the three lines coincide, and this non-split curve is described by the function

$$y_1 = 3Ae^{-(x/b)^2}, \tag{9}$$

where x represents the wavelength (choosing the origin at the center of the π component) and A represents the amplitude of one single component. We assume the three components have the same amplitude. The curve given in Eq. (9) has a FWHM width W of

$$W = 2b\sqrt{\ln(2)}. \tag{10}$$

Now consider that the two σ components are shifted an amount Δ to either side of the origin. We also inflate the amplitude by an empirical factor F. Then the total profile has the form

$$y_2 = FAe^{-(x+\Delta)^2/b^2} + FAe^{-x^2/b^2} + FAe^{-(x-\Delta)^2/b^2}. \tag{11}$$

Figure 6 shows a plot of this function, for different values of Δ and F. When analyzing the spectra, F must be adjusted separately for each spectral line, in order to match the slopes

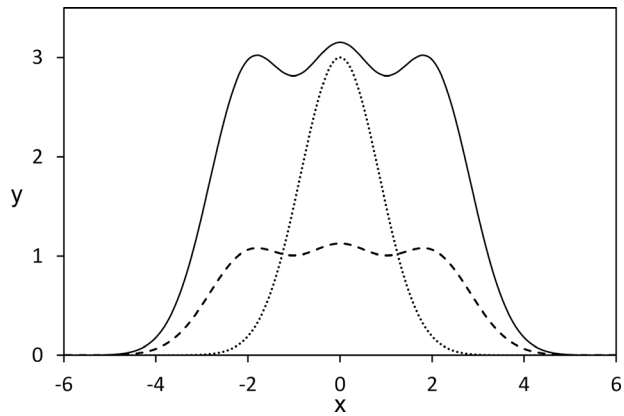

Fig. 6. Sum of three Gaussian spectral lines of width $W = 2$. Dotted curve: Sum of three non-displaced profiles ($\Delta = 0$), modeling the spectral line without magnetic field as in Eq. (9). Dashed curve: Sum of the same profiles with a displacement of $\Delta = 2$, representing the same spectral line now split by the Zeeman effect. Solid curve: The same as the dashed curve but inflated by a factor $F = 2.8$ as in Eq. (11) to match the slope of the original (dotted) profile.

of both sides. Fortunately, this F does not enter the calculation.

To compute the slopes, we take the derivative of Eq. (9) and evaluate it at $x_1 = -b\sqrt{\ln(2)} = -W/2$, where the function has the value $y_1 = 3A/2$ (at half maximum), which gives

$$\frac{dy_1}{dx} = -\frac{2xy_1}{b^2} = \frac{3A\sqrt{\ln(2)}}{b}. \tag{12}$$

Likewise, the derivative of Eq. (11) is

$$\frac{dy_2}{dx} = -\frac{2xy_2}{b^2} - \frac{2y_2\Delta}{b^2}H, \tag{13}$$

where the function $H(x, \Delta, b)$ is defined by

$$H = \frac{e^{-(x+\Delta)^2/b^2} - e^{-(x-\Delta)^2/b^2}}{e^{-(x+\Delta)^2/b^2} + e^{-x^2/b^2} + e^{-(x-\Delta)^2/b^2}}, \tag{14}$$

and simplifies to

$$H = \frac{e^{-2x\Delta/b^2} - e^{2x\Delta/b^2}}{e^{-2x\Delta/b^2} + e^{2x\Delta/b^2} + e^{\Delta^2/b^2}}. \tag{15}$$

In order to equalize the slopes at a single height, the derivative dy_2/dx in Eq. (13) should be evaluated at a point x_2 where $y_2 = 3A/2$. This point occurs at $x_2 = -b\sqrt{\ln(2)} - \delta$, where we define $\delta = x_1 - x_2$ as the (measured, one-side) broadening of the spectral line. Equating the two derivatives we obtain

$$\frac{3Ab\sqrt{\ln(2)} + 3A\delta}{b^2} - \frac{3A\Delta}{b^2}H(x_2, \Delta, b) = \frac{3A\sqrt{\ln(2)}}{b}, \tag{16}$$

which simplifies to give

$$H = \frac{\delta}{\Delta}. \tag{17}$$

In other words, $H(x_2, \Delta, b)$ is the inverse of the correction factor that must be applied to the measured broadening δ in order to obtain the true wavelength shift Δ. Now, evaluating H from Eq. (15) at $x_2 = -b\sqrt{\ln(2)} - \delta$, using Eqs. (10) and (17), and defining the dimensionless quantities

$$q \equiv \frac{\delta}{W} \quad \text{and} \quad Q \equiv \frac{\Delta}{W}, \tag{18}$$

we obtain the relation

$$\frac{q}{Q} = H = \frac{e^{4Q(1+2q)\ln(2)} - e^{-4Q(1+2q)\ln(2)}}{e^{4Q(1+2q)\ln(2)} + e^{-4Q(1+2q)\ln(2)} + e^{4Q^2\ln(2)}}. \tag{19}$$

This equation embodies the relation between the dimensionless line broadening q and the dimensionless wavelength shift Q, and must be solved for Q when q is known from observation. Solving Eq. (19) for Q must be done numerically, but several approximations are possible.

When $Q > 1$ the wavelength shift is greater than the line width and the Zeeman splitting is resolved. In this case, one would expect Eq. (19) to approach the identity function $q = Q$ because there would be no broadening; δ would directly measure (be equal to) the Zeeman shift. The numerical solution confirms this hypothesis. On the other hand, when $Q < 1$ we find that q is considerably smaller than Q, in fact close to Q^2.

Figure 7 shows the numerical solutions (points) to Eq. (19), with q plotted as the independent variable, since it is found from observations. These results clearly exhibit the resolved ($Q > 1$) and the unresolved ($Q < 1$) regimes. Measurements made with ESPARTACO are located in the unresolved region, where a correction must be applied. An instrument with greater spectral resolution will yield smaller line widths W, resulting in greater values of q, thus moving the observations from the correction zone closer to the linear zone.

For small values of q, the points in Fig. 7 can be fitted to the square-root relation

$$Q = 0.83\sqrt{q}, \tag{20}$$

(drawn in Fig. 7 with a solid curve) or equivalently, in terms of measured quantities,

$$\Delta\lambda = 0.83\sqrt{W\delta}. \tag{21}$$

An even better fit may be constructed as

$$Q = 0.87q^{0.54}, \tag{22}$$

but such accuracy is not needed, as our measured data show a high degree of uncertainty. Therefore Eq. (20) is preferable for its simplicity.

V. ESPARTACO SUNSPOT SPECTRA

During 2011, near the maximum of solar activity, several sunspot spectra with ESPARTACO were made. For each spectrum in the umbra of a prominent sunspot, a reference spectrum was also taken outside the spot. Useful data were obtained on June 22, September 5, and September 12, and were located, respectively, in Active Regions 1236, 1283, and 1289. The spectra cover several wavelength ranges. After calibrating the wavelength scale, the width W of a number of lines (in wavelength units) was measured. The sample included some lines previously targeted on account of their large Landé factor. Other lines turned out to be

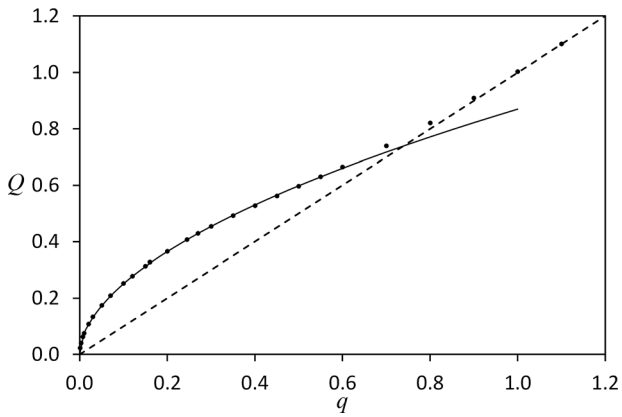

Fig. 7. Solutions to Eq. (19). The dots mark the exact numerical solutions, which approach asymptotically the identity function (dashed line). The solid curve shows the square-root approximation given in Eq. (20).

noticeably broadened, while still others stood out clearly in the spectrum and allowed for a precise measurement. Widths are typically a tenth of an Angstrom.

Next, the method explained above was used to measure the broadening (δ) for each line, up to a few milli-Angstroms (mÅ). For all measured spectral lines, a value of $q < 0.4$ was found. But the method for obtaining Q and then $\Delta\lambda$ was designed for lines that were split into triplets. Therefore, the triplet transitions needed to be manually isolated. Thus, all observed spectral lines were found in the NIST database,[12] which gives the quantum numbers of both levels involved in a transition, and triplet lines were selected (having $J = 0$ in one level, or the same g in both levels).

Only the September 5 spectra contained a considerable number of triplets. The three spectra obtained that day, each being some 50-Å long and centered at 5236 Å, 6161 Å, and 6290 Å, gave a total of 32 measurable lines, noticeably broadened, including 12 triplets and 20 non-triplets. (The three spectra from September 5 are available in supplementary material.[11])

For the triplets, $\Delta\lambda$ was found as described above, using the exact numerical solution. Figure 8 shows the results plotted against $G\lambda^2$, which, according to Eq. (7), should give a linear relationship. For the error estimations, an uncertainty of 3 mÅ was assumed in all broadenings (δ) based on the typical accuracy of the measurements; no error in the line widths (W) was considered because these values are larger and, consequently, their relative uncertainty is smaller. For unknown reasons, the scatter is larger than one would expect from the error bars, and a complete two-parameter linear fit would not pass through the origin at all. This high dispersion hints at the imprecision of the method; the error estimate might be too optimistic, but there could also be unknown systematic errors.

The slope of the plot shown in Fig. 8 yields the magnetic field according to

$$B = 4\pi c \frac{m}{e} \frac{\Delta\lambda}{G\lambda^2}. \tag{23}$$

Using the September 5 data, we find $B = 1620 \pm 160$ G. This result is comparable to the data from the HMI instrument[3] on the Solar Dynamics Observatory (SDO),[4] which takes solar images of almost 4000 pixels diameter and gives the magnetic field for every pixel (measured using a polarization method). The maximum HMI field strength of the observed sunspot is 2420 G. Our observations yield 2/3 of this value, which is understandable in view of the lower spatial resolution (here the maximum field value covers only a very small portion of the sunspot, while ESPARTACO averages the field over a larger area).

There is no equivalently simple way of obtaining $\Delta\lambda$ from δ for the non-triplet lines. A theoretical relation similar to Eq. (19) should be developed for each splitting scheme. But an approximate relation is suggested in Eq. (21), in that non-triplets might obey a square-root approximation, with a suitable coefficient (not necessarily 0.83). The September 5 observations were used to calibrate such a model. Since a single sunspot was observed, triplets and non-triplets should give the same magnetic field. In order to equate the non-triplet slope to the triplet slope, a coefficient of 0.72 is needed; thus, for non-triplets,

$$\Delta\lambda = 0.72\sqrt{W\delta}. \tag{24}$$

Figure 9 shows the resulting plot of $\Delta\lambda$ vs $G\lambda^2$, which shows a fairly linear trend. The scatter and error bars show more coherence than in Fig. 8, and a complete two-parameter linear fit does indeed pass quite close to the origin.

Next, Eq. (23) was applied to the June 22 and September 12 spectra, obtaining the following results. The June 22 spectra were low-quality and only 2 lines, non-triplets, proved useful, giving $B = 1900 \pm 100$ G. For comparison, the HMI peak field is B = 2880 G. Again our result is approximately 2/3 of the peak value. For September 12 there are 2 triplets and 5 non-triplets. The triplets give $B = 1440 \pm 340$ G, and the non-triplets give $B = 1430 \pm 170$ G. The similarity of these separate results validates the value 0.72 for the coefficient in Eq. (24). The overall result for September 12 is $B = 1440 \pm 140$ G. The HMI gives a maximum field of 2890 G. In this case, our measurement gave only half the peak value, which may be because the sunspot was divided in two by a narrow line where the field is much weaker (see Fig. 10). This cleft is likely to have contributed significantly to the observed field.

VI. OXYGEN LINES

One of the September 5 spectra includes a number of atmospheric oxygen lines around 6300 Å (see Fig. 1), which

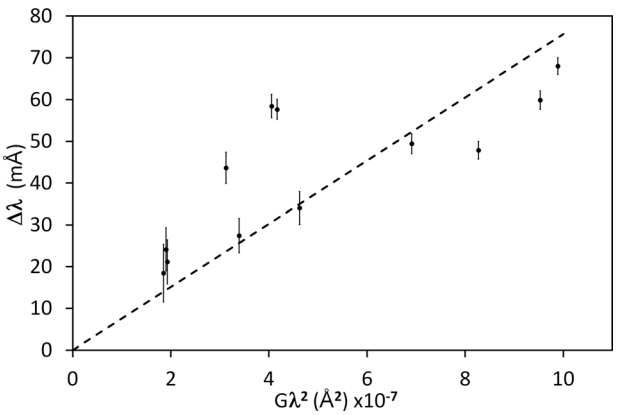

Fig. 8. Zeeman splitting $\Delta\lambda$ vs $G\lambda^2$ for all September 5 triplets. The $\Delta\lambda$ values were computed numerically using Eq. (19). The dashed line represents the best linear fit through the origin.

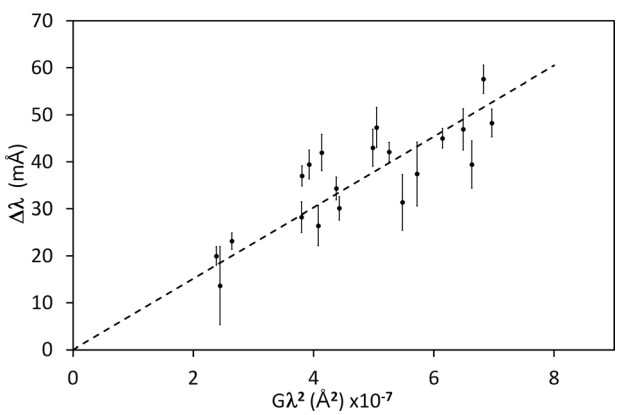

Fig. 9. Zeeman splitting $\Delta\lambda$ vs $G\lambda^2$ for all September 5 non-triplets. The $\Delta\lambda$ values were computed using the square-root approximation with the coefficient 0.72. The dashed line represents the best linear fit through the origin.

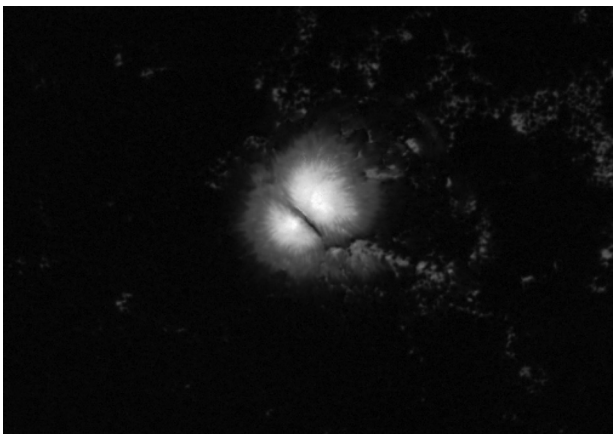

Fig. 10. Sunspot observed on September 12, 2011. On this HMI magnetogram, the brightness is proportional to the magnetic field.

should have $\Delta\lambda = 0$. In order to assess the reliability of the method, the same technique was applied to 11 of these telluric lines. The resulting mean $\Delta\lambda$ is

$$\overline{\Delta\lambda} = -1.8 \pm 9.5\,\text{mÅ}. \tag{25}$$

The mean value of these experimental $\Delta\lambda$ is satisfactorily small, although the dispersion is quite large. This dispersion is similar to that of the solar lines, which (for September 5) show a vertical dispersion of 14.9 mÅ (for triplets) and 6.4 mÅ (for non-triplets).

VII. CONCLUSIONS

We have seen that it is possible to obtain realistic values for solar (sunspot) magnetic fields using spectra that are inadequate for precise measurements. Besides a review of atomic and quantum physics, and more specifically the Zeeman effect, this exercise involves creative data handling (how do you measure line broadening on very noisy spectra?) and theoretical modeling for a specific problem (how do you compute the splitting value from measured line broadening?). We believe this exercise makes a useful project for undergraduate students; it will deepen their theoretical knowledge and give them practice with data acquisition, reduction, and analysis.

This exercise illustrates how reasonable results can be wrung from data obtained with equipment that is actually insufficient (a situation that is often found in science, particularly at the frontier of discovery). Students (and the general public) should appreciate that observed results are not always as pristine, clear-cut, and straightforward as often supposed.

Perhaps the worst problem with the instrumentation used is the modulation of the continuum, which hampers the measurement of unambiguous broadening values. This effect is stronger when the light entering the fiber is more collimated. When the fiber is pointed at a cloudy sky, very fine spectra result. But in order to single out a sunspot, a telescope is needed, collimating the light and aggravating the modulation. A more adequate optical setup might mitigate this problem. Another approach might involve flat-field images taken through the spectrograph. A third way could be to smooth out the actual spectra, blotting out the absorption lines, and using the result as "flats." However, neither tactic has yet proven satisfactory.

Students are invited to draw up and try out improved observation techniques (in order to get better quality spectra), improved image reduction techniques (to get rid of the modulation of the continuum), better ways to measure line broadening, and computing analytical models for non-triplet splitting schemes. Experiments with known laboratory fields might be useful. Finally, they might wish to tackle spectra from magnetic stars.

ACKNOWLEDGMENTS

The author would like to thank the reviewers for their useful and valuable corrections and suggestions.

[1]G. Mathys *et al.*, "The mean magnetic field modulus of Ap stars," Astron. Astrophys. Supp. **123**(2), 353–402 (1997).
[2]B. W. Lites and A. Skumanich, "Stokes profile analysis and vector magnetic fields. V. The magnetic field structure of large sunspots observed with Stokes II," Astrophys. J. **348**, 747–760 (1990).
[3]P. H. Scherrer *et al.*, "The helioseismic and magnetic imager (HMI) investigation for the solar dynamics observatory (SDO)," Solar Phys. **275**, 207–227 (2012).
[4]Solar dynamics observatory, <http://sdo.gsfc.nasa.gov/>.
[5]Benjamin Oostra, "ESPARTACO: A low-cost, high-resolution spectrograph for students," Rev. Colomb. Fís. **43**(2), 312–317 (2011); available at http://revcolfis.org/ojs/index.php/rcf/article/view/430224/pdf.
[6]Benjamin Oostra, "Measurement of the earth's rotational speed via Doppler shift of solar absorption lines," Am. J. Phys. **80**(5), 363–366 (2012).
[7]E. F. Borra and D. Deschatelets, "Measurements of stellar magnetic fields using autocorrelation of spectra," Astronom. J. **150**(5), 146–155 (2015).
[8]E. Landi Degl'Innocenti and M. Landolfi, *Polarization in Spectral Lines* (Springer, Dordrecht, Netherlands, 2004), p. 90.
[9]VALD (Vienna Atomic Line Database), <http://www.astro.uu.se/~vald/php/vald.php>.
[10]Spectroweb, <http://spectra.freeshell.org/whyspectroweb.html>.
[11]See supplementary material at http://dx.doi.org/10.1119/1.4975109 for our spectra from September 5, from inside and outside the sunspot and covering three wavelength ranges.
[12]NIST atomic spectra database, <http://www.nist.gov/pml/data/asd.cfm>.